
EVOLUTIONARY SCHEMES FOR PROTOSTARS, PROTO BROWN DWARFS AND THEIR ENVIRONMENTS

M. D. SMITH

Armagh Observatory, College Hill, Armagh, N. Ireland, BT61 9DG

ABSTRACT. The evolutions of protostars, envelopes, disks, jets and outflows may be closely linked. I review, update and extend the Unification Scheme, which links these components through simple redistributions of mass and energy. This yields predictions and correlations between parameters such as outflow size, outflow momentum, disk mass, bolometric luminosity and envelope mass. Evolutionary tracks are derived.

Inflow and outflow problems are tackled. A steady disk can digest the infalling gas only if the envelope's centrifugal barrier lies within about 20 AU. The high mechanical luminosities and thrusts from the youngest (Class 0) protostars imply high outflow efficiencies. In the model, high jet speeds allow the disk angular momentum and accretion luminosity to be expelled within the jets during the early Class 0 stage (consistent with the magneto-centrifugal wind mechanism). The momentum crisis is solved even when the jet flow is ballistic: momentum is transferred to the ambient gas via wide bow shocks rather than just through the direct jet impact.

In Class 1 sources, turbulence-driven accretion mechanisms negotiate the lower inflow rates and so the outflows are less efficient. The ambient medium decelerates the leading bow shock, limiting the outflow growth to a few parsecs, and further reducing the mechanical luminosity. The scheme successfully explains the evolution of jet structure and molecular content. Pulsations in dense ballistic molecular jets give way to fluid instabilities in light atomic jets.

1. INTRODUCTION

Protostars and young stars of quite low mass, which may become stars like our Sun, are classified by how deeply they are obscured (Lada 1987; André, Ward-Thomson & Barsony 1993; 2000). An evolutionary sequence along which the obscuration decreases is suggested. This could be perceived as the record of the conversion of a dust-obscuring cloud into a star through collapse. The picture, however, must be more complex since a cloud spins and its angular momentum is sufficient to hold up an infall. A question raised is: where is the angular momentum deposited?

Jets and bipolar outflows are supersonic streams of gas within quite narrow confines (see reviews by Eislöffel *et al.* 2000; Richer *et al.* 2000). They are commonly found with protostars and often help to locate the most deeply embedded. They are classifiable by their power, thrust, mass, size and constitution (Völker *et al.* 1999). Jets may evolve from a ballistic and molecular phase into a light and atomic phase. Outflows may evolve from small and high thrust to giant but low thrust. A second question raised is: are the jets responsible for extracting the angular momentum (Königl & Pudritz 2000)? It remains extremely difficult to detect spinning jets although Davis *et al.* (2000) do present some evidence. But if so, then we can expect the outflow evolution to be synchronised with the inflow.

Outflow ages had been thought to be generally too low for a simultaneous evolution with a protostar to be possible. An outflow of linear size 0.3 parsecs would form in just $\sim 3,000$ years with an expansion rate of 100 km s^{-1} . This has now changed: many outflows are indeed several parsecs long and show evidence for deceleration near the extremities, extending the apparent age of the oldest to over 100,000 years (Bally & Devine 1994; Eislöffel & Mundt 1997).

The highly-obscured Class 0 protostars are probably present for a period of only 10,000 years, on going by the observed number (André *et al.* 2000). The Class 1 protostars, seen in the infrared, are estimated to be of order 100,000 years. Class 2 protostars lack a protostellar envelope but still possess an optically thick disk. These are the Classical T Tauri stars, of order 10^6 years old. The interpretation of these classes as a sequence is not fully established. For example, it is not clear that all stars pass through a Class 0 stage.

We here review and extend the Unification Scheme which unites the phases of the obscuring envelope, accreting disk, protostar, jet and outflow. The model assumes a mass inflow rate and a jet outflow speed. All the other quantities are then derived by making simple assumptions concerning the physics and dynamics, mainly following the redistribution of the mass. The most important assumption that proves necessary is that there is a stage, corresponding to the Class 0 stage, during which the jet outflow is particularly efficient ($\sim 40\%$ of the accreting mass is ejected) in comparison to the other stages ($\sim 10\%$ ejected).

This aims of the work are:

- to predict the evolutionary tracks on standard diagrams so that we can estimate protostellar ages,
- to determine the distinguishing features as a function of age or stage (e.g. are molecular jets associated with Class 0 protostars?),
- to differentiate between inflow scenarios (e.g. is viscosity through self-gravitational forces dominant in some phase?),
- to test the need for alternative physics (is the mass always accreted through the disk?),

- to explain the nature of old outflows (the original motivation),
- to develop a framework within which to discuss further observational properties such as maser evolution and accretion shocks.

The initial model (Smith 1999) concentrated on the jet and outflow, and assumed a constant fraction of ejected mass. The evolution of jets from ballistic and molecular to light and atomic was predicted. The second version discussed the type of accretion, finding the need for an abrupt accretion phase (Smith 2000a). The mass-radius relation for the protostellar core was investigated and found to be consistent with detailed derivations, although large uncertainties exist in our knowledge. The third version first studied the evolutionary tracks, establishing the need for a mass outflow efficiency dependent on the mass inflow rate (Smith 2000b). An ambient medium was also included to decelerate the jets by ram pressure and so interpret outflow ages and sizes. The present version is more or less complete, bringing in the accretion disk and envelope evolutions.

Our scope is still very limited. We consider the formation of single objects only. We do not explore the many possible variations and extensions of the model. And we consider only continuous evolutions, rather than several outbursts.

2. THE MASS INFLOW

2.1. Accretion rate

Each star formation scenario must assume initial conditions in a dense core or ‘envelope’. This determines the subsequent evolution only so far as the system is isolated. Small-scale phenomena, such as planet formation, which depend on turbulence or instabilities which lead to fragmentation, cannot be forecasted.

The initial conditions are here expressed in one equation for the rate at which the envelope loses mass to the disk, protostar and outflow. As shown by Foster & Chevalier (1993), isothermal isotropic collapse of cores supported by thermal pressure yield infall rates of the form $\dot{M}_a = f(t) [c_s^3/G]$. The function $f(t)$ can be anything from gradually decreasing over a time $\sim 200\tau$ to a sharply peaked function at time $\sim 0.1\tau$. The time and mass flow scales are

$$\tau = 1/\sqrt{(4\pi G\rho_c)} = 1.3 \cdot 10^5 \left[\frac{7.6 \cdot 10^{-20} \text{ g cm}^{-3}}{\rho_c} \right]^{1/2} \text{ yr} \quad (1)$$

$$\frac{c_s^3}{G} = 1.6 \cdot 10^{-6} \left[\frac{c_s}{0.19 \text{ km s}^{-1}} \right]^3 \text{ M}_\odot \text{ yr}^{-1} \quad (2)$$

where ρ_c is the initial central density and c_s is the sound speed. Inclusion of envelope spin, turbulence, magnetic field and fragmentation would introduce further initial parameters (see reviews by André *et al.* 2000; Calvet, Hartmann & Strom 2000).

2.2. Exponential models

Bontemps *et al.* (1996) and Myers *et al.* (1998) assume that the envelope loses mass proportional to its mass, $\dot{M}_a = -\dot{M}_{env} \propto M_{env}$. This leads to an exponentially decreasing envelope mass and accretion rate,

$$M_{env}(t) = M_o e^{-t/\tau_f}, \quad (3)$$

$$\dot{M}_a(t) = \frac{M_o}{\tau_f} e^{-t/\tau_f}, \quad (4)$$

but begins with an established high accretion rate. An alternative exponential model allows for a rapid rise and fall by modelling

$$\dot{M}_a(t) = \dot{M}_o e^{2(\tau_r/\tau_f)^{1/2}} e^{-\tau_r/t} e^{-t/\tau_f}, \quad (5)$$

and we can put $\tau_r = 0$ if desired. The maximum accretion rate \dot{M}_o occurs at time $t_m = \sqrt{(\tau_r \tau_f)}$.

2.3. Constant rate models

Constant accretion models have been favoured since the work of Shu (1977) on singular isothermal spheres. It is clear, however, that the rate must eventually fall (Hartmann 1998). One can take a period of constant accretion followed by an equally long transition period in which the rate falls to zero (Lin & Pringle 1990).

2.4. Power law models

Here, as in Smith (1999), we take a sharp exponential rise and a power law decrease in time. In rough, we imagine that the power law will provide an early peak in which $\dot{M}_a = 10^{-4} \text{ M}_\odot \text{ yr}^{-1}$ for 10^4 years, and eventually becoming $\dot{M}_a = 10^{-7} \text{ M}_\odot \text{ yr}^{-1}$ for 10^6 years, corresponding to Class 0 and Class 2 or Classical T Tauri stars, respectively. The power-law has substantial observational support (Calvet *et al.* 2000). High-mass stars would possess accretion rates 10-20 times higher. This enables us to model scenarios corresponding to either a variable accretion speed or a feedback mechanism in which the outflow enhances the envelope break up which is then expelled or accreted at a higher rate. Our aim is to determine the consequences of an assumed \dot{M}_a , and so test the underlying physics.

We choose the accretion rate to take the form

$$\dot{M}_a(t) = \dot{M}_o (\epsilon/\alpha)^\alpha (t/t_o)^{-\alpha} \exp(-t_o/t). \quad (6)$$

This has a sharp exponential rise to \dot{M}_o and a power law fall-off. A constant-accretion model corresponds to $\alpha \sim 0$ and t_o small, gradual-accretion corresponds to $\alpha \sim 0.5$ and abrupt accretion to $\alpha \sim 2 - 3$.

The envelope evolution can be written analytically in terms of an incomplete Gamma function on integrating Equation 6:

$$M_{env}(t) = \dot{M}_o t_o (\epsilon/\alpha)^\alpha [1 - \Gamma(\alpha - 1, t_o/t)]. \quad (7)$$

3. THE ENVELOPE AND DISK

We assume an initial envelope mass M_{env} . Mass is lost from the envelope into a circumstellar disk. The disk is ‘viscous’. The gas reaches an inner accretion disk at the same rate as with which it is supplied by the envelope. The inner accretion may be non-steady, the gas either being expelled in the jets or accumulated onto the surface of a hydrostatic core, later to become the star itself. The disk mass is thus proportional to the accretion rate and the accretion time scale.

We take simple envelope properties in this version. A typical outer disk radius would be 500-1000 AU (Pringle 1988, Bodenheimer 1992) as given by the centrifugal barrier. We here

assume a disk of diameter 1000 AU and an inner envelope radius $R_e = 500 \text{ AU}$. We calculate an optical depth of the envelope τ_e assuming a spherical density structure with $\rho \propto R^{-3/2}$. We avoid calculating the outer envelope radius (where the envelope merges into the ambient cloud) by assuming it is simply ϕR_e and taking ϕ constant ($\phi = 3$). The inner density is then

$$\rho_e = \frac{3M_{env}}{8\pi R_e^3(\phi^{3/2} - 1)} \quad (8)$$

and the envelope optical depth is

$$\tau_e = 2\kappa\rho_e R_e(1 - \phi^{-1/2}) \quad (9)$$

where we follow Myers *et al.* (1998) and take the emissivity at $12\mu\text{m}$ as $\kappa = 4 \text{ cm}^2 \text{ g}^{-1}$.

Standard turbulent viscosity is only efficient at separating the angular momentum from the mass out to radii of about 100 AU for the initial rapid accretion rates from the envelope. Hence massive outer disks build up until the viscous mechanisms associated with self gravity are effective. This could lead to the formation of secondary objects (stars, brown dwarfs), and so cut off the jet supply line. Perhaps more likely is that high accretion rates lead to simultaneous binary formation and powerful molecular jets.

We assume the disk processes the material fast and so remains steady. The outer part of the disk will lag behind. The outer radius of the steady state disk can be found by requiring the disk accretion time scale $t_\nu(R) = R^2/\nu$ to be less than the time scale for changes in the accretion rate \dot{M}_a/\dot{M}_a . This yields a steady disk extent R_s .

The disk temperature T_d and sound speed c_d are given by standard expressions for an optically thick and isothermal structure (Pringle 1981). The accretion energy is radiated locally:

$$T_d^4(R, t) = \frac{3GM(R, t)\dot{M}_a(t)}{8\pi\sigma R^3} \left[1 - \left(\frac{R_*}{R} \right)^{\frac{1}{2}} \right], \quad (10)$$

where R_* is the protostellar radius and $M(R, t) = M_*(t) + M_d(R, t)$ is the sum of the protostellar and disk mass internal to R . The sound speed for a molecular gas disk with a mean molecular weight of 2.3 is $c_d = 6.01 \cdot 10^3 T_d^{1/2} \text{ cm s}^{-1}$.

The disk mass M_d is not expressible analytically since the accretion is driven by two viscosity components with differing functional forms. First, we take the usual turbulent viscosity $\nu_t = \alpha_d c_d H$ where H is the disk thickness and α_d is a dimensionless parameter which we set to 0.1 unless otherwise stated (Shakura & Sunyaev 1973). This yields

$$\nu_t = \frac{2\alpha_d c_d^2}{3\Omega}, \quad (11)$$

where the angular rotation speed is $\Omega = \sqrt{GM/R^3}$. The component of viscosity related to self-gravitational forces is parameterised, as suggested by Lin & Pringle (1987):

$$\nu_g = \frac{2\mu_d c_d^2}{3\Omega} \left(\frac{Q_c^2}{Q_t^2} - 1 \right) \quad (12)$$

for $Q_t < Q_c$ and $\nu_g = 0$ otherwise. Here, the efficiency parameter μ_d and the instability parameter Q_c will also be set to unity (see Lin & Pringle 1990). Hence, the parameter

$$Q_t = \frac{c_d \Omega}{\pi G \Sigma} \quad (13)$$

determines the importance of viscosity through the disk's own gravity. Note that the viscosity can be determined by self-gravity even when the protostellar mass is large when the disk column density is large. This may well arise where the turbulent viscosity is inefficient, in the outer disk regions, leading to a build up of mass until self-gravity takes effect.

The disk column is given by

$$\Sigma = \frac{1}{2\pi R} \frac{dM}{dR} \quad (14)$$

and the cumulative mass distribution

$$\frac{dM}{dR} = \frac{R \dot{M}_a}{\nu_t + \nu_g} \quad (15)$$

is given by the viscosity. This completes the set of equations which is integrated from an inner radius to yield the full disk structure. From the disk column it is straightforward to calculate the disk radius at which the optical depth is unity, $R_{\tau=1}$.

4. THE MASS AND ENERGY BIFURCATION

4.1. The protostar

The efficiency ϵ of mass diversion from inflow to outflow, from disk to jets, reflects the disk-wind model. The magneto-centrifugal model may be quite efficient and ϵ can reach the thirty per cent level in the x-wind model (Shu *et al.* 1994). In fact, such magneto-centrifugal winds can carry away the total angular momentum and kinetic energy of the accreting disk material (see Hartmann 1998).

Previously, we found that a constant efficiency fails to explain the observational facts (Smith 2000b). The Class 0 outflows appear to have a mechanical luminosity of order of the bolometric luminosity of the protostellar core. On the other hand, Class 1 outflows have mechanical luminosities typically about a factor of 10 lower (see Figure 5). With the same mass outflow efficiency, this would then require that the *jet speed* is higher in Class 0 outflows. This is, however, contrary to the observations which associate lower velocities ($\sim 100 \text{ km s}^{-1}$) to the Class 0 outflows. Theoretically, a higher speed combined with the high mass outflow rate require deeper gravitational potential wells (high speed jets, such as on the solar surface, can only occur locally over short time spans). This does not seem plausible given that electron degeneracy pressure will limit the collapse of the growing hydrostatic core. Even if possible, the deeper well simultaneously increases the accretion luminosity, maintaining a constant ratio of outflow to bolometric powers. This argues for an evolving mass efficiency.

To simulate the Class 0 episode, we adopt for the fraction of mass ejected in the jets

$$\epsilon = \eta \left[\frac{\dot{M}_a(t)}{\dot{M}_o} \right]^\zeta \quad (16)$$

where $\zeta = 1$ has been assumed to date. Hence the mass left over which accretes on to the core to form the star is

$$M_*(t) = \int_0^t (1 - \epsilon) \dot{M}_a. \quad (17)$$

Finally, the crucial assumptions are completed by adopting a protostellar radius which is consistent with an increasing jet speed with time, and consistent with our knowledge of protostellar core evolution. Mass-radius tracks were obtained by Smith (2000a) on employing

$$\frac{GM_*(t)}{R_*(t)} = \psi \exp\left(-\frac{t_1}{2t}\right) \quad (18)$$

to determine R_* with t_1 a constant and a jet speed

$$v_j = v_f \exp(-t_1/t). \quad (19)$$

We fix the jet speed proportional to the protostellar escape speed:

$$v_j = \chi \left(\frac{GM_*}{R_*}\right)^{1/2}. \quad (20)$$

(which thus fixes ψ . Although these are big working assumptions, partly justified by the sparse observations and partly by the most naive theoretical explanations, they should suffice to produce a scheme from which we can make predictions, observations and then revamp our model.

With $\eta \rightarrow 1.0$ & $\chi(t) = 1$, the jet power approaches the total accretion luminosity in bringing the gas in to the stellar surface during the peak accretion phase. More consistent with the theory, however, would be a peak outflow efficiency of $\eta \sim 0.1 - 0.5$ combined with a terminal jet speed of a few times the escape speed $\chi \sim 2 - 4$.

4.2. The jets

Identical twin jets are adopted. The jets may well be atomic at their origin, although fast-moving molecular maser spots appear within 10 AU. The density in the jets ρ_j , assumed smooth, is given through

$$\rho_j = \frac{\epsilon \dot{M}_a}{2\pi r_j^2 v_j} \quad (21)$$

which yields hydrogen nuclei densities (in cm^{-3}) of

$$n_j = 4.3 \cdot 10^3 \frac{\epsilon \dot{M}_a}{10^{-6} M_\odot \text{yr}^{-1}} \left(\frac{10^2 \text{ km s}^{-1}}{v_j}\right) \left(\frac{10^{16} \text{ cm}}{r_j}\right)^2, \quad (22)$$

where a ten per cent helium abundance is taken and r_j is the jet radius. The radius corresponds to a distance of $D_j = 10^{17}$ cm for a jet with a 12° total opening angle. This opening angle is chosen to correspond to the angle of the tunnel drilled by the jets, assuming the jet to occupy the whole tunnel. If it corresponds to a precession angle, the jet would occupy less of the tunnel volume. This is relevant to the chemistry which depends on the density but not to the ram pressure argument which depends on the average applied thrust.

Atomic and molecular jets are observed, but are not mutually exclusive. Molecular jets can be observed from the youngest protostars while atomic jets are observed at optical wavelengths from some Class I and later young stars. Molecular hydrogen formation in a jet requires (1) the presence of dust on which to form, (2) high densities to produce a high encounter rate and (3) the time to cool so as not to dissociate through reformation heating. To cool below ~ 4000 K takes

about $t_d = 2 \cdot 10^6$ seconds, (the inverse of the average Einstein coefficient for vibrational transitions). This implies that H_2 jets may not be detectable until a distance of $D_r = 2 \cdot 10^6 v_j$. Given a reformation time scale of $t_r = 10^{17}/(\theta n_j)$, (where θ is the fraction of dust relative to an average cloud value) then yields an estimate for the molecular hydrogen number fraction as

$$f = \frac{t_d}{t_r + 2t_d} \quad (23)$$

evaluated at D_r and a full compliment of dust ($d = 1$).

The jet magnetic field strength measures the field necessary to drive an outflow. It equates the Lorentz and gravitational forces within the jet, assumed to be poorly collimated near the stellar surface (see Fendt & Camenzind 1996). It is also equivalent to equating the Alfvén speed to the escape speed within the outflow near the protostar. We plot in the Figures

$$B = \left[\frac{\epsilon \dot{M}_a GM_*}{v_j R_*^3} \right]^{\frac{1}{2}}. \quad (24)$$

Techniques to detect surface magnetic fields of the predicted strength are now available (e.g. Guenther *et al.* 1999).

4.3. The bipolar outflow

There may be a considerable time lag between the ejection of gas in the jets and the transformation of the bulk kinetic energy into infrared or submillimetre radiation. The infrared lag will depend on the distance between the protostar and the jet or bow shocks. We here assume that the infrared energy is mainly dissipated within warm shocks at the termination bows. For simplicity, take an external medium of constant density n_{ext}

We assume the jet opening angle remains constant, i.e. the jet is hypersonic and the surrounding cocoon is unable to curtail the free expansion. The size of the outflow is then given by a ram pressure argument. The outflow expands at a speed

$$v_{ext} = \frac{v_j}{1 + (n_{ext}/n_j)^{1/2}}. \quad (25)$$

to yield the linear half-size $D = d/2$:

$$D(t) = \int_0^t v_{ext} dt. \quad (26)$$

These two factors determine the apparent rate at which the mechanical energy and momentum are accumulated in the bipolar outflow:

$$2L_{mech}(t) = \left[\int_0^t \epsilon \dot{M}_a v_j^2 dt \right] / (D/v_{ext}). \quad (27)$$

$$F_{mech}(t) = \left[\int_0^t \epsilon \dot{M}_a v_{jet} dt \right] / (D/v_{ext}). \quad (28)$$

Note that the mechanical luminosity is identical to the full accumulated jet energy. For the full thrust and energy to be transmitted to a lower density external medium during the ballistic flow stage requires a process additional to ram pressure. It should be noted that the *direct* impact of the jet drives the external gas to almost the jet speed, but the low density implies an efficiency of momentum transfer of only $\sim n_{ext}/n_{jet}$.

Table 1. The parameters employed in all figures which employ the power-law accretion rate given by Equation 6.

Quantity	Fiducial Value	Origin
t_o	20,000 yr	mass flow time scale
t_1	60,000 yr	jet speed time scale
α	2.0	mass rate power law index
α_d	0.1	turbulent disk index
Q_c	1.0	self-gravity viscosity
η	0.4	maximum jet efficiency
χ	2.12	jet speed factor
v_f	$4.5 \cdot 10^7 \text{ cm s}^{-1}$	final jet speed
θ	1.0	dust mass (per cent)
n_{ext}	$1.0 \cdot 10^3 \text{ cm}^{-3}$	ambient density
κ	$4 \text{ cm}^2 \text{ g}^{-1}$	emissivity at $12\mu\text{m}$

However, the observed outflows could simply be formed from the jet molecular material during the ballistic stage, requiring no transfer. This is clearly only possible provided the CO molecule has formed along with the H_2 .

Subsequent to the impact, the jet gas flows into a narrow shear layer close to the edge of the leading bow shock itself: a wide bow structure occurs. The extended bow is pushed through the external medium, redistributing the jet momentum over the bow area. This scenario is confirmed by numerical experiments which demonstrate that the momentum is predominantly carried at the highest flow speeds (i.e. the mass index $\gamma > -2$, Smith, Suttner & Yorke 1997). The CO line profiles derived numerically from ballistic simulations demonstrate a continuous transfer of momentum from high jet speeds to low speeds. There is no deep ridge in the profiles and no *accumulation* of momentum into a jet velocity ‘spike’).

5. RESULTS: THE DISK AND ENVELOPE

Having set up the evolutionary equations for the five components, we now present and compare the evolutions. First, we look at the evolution of the disk’s radial profile, as displayed in Figure 1 for three crucial ages: 10^4 yr (peak accretion), 10^5 yr (transition) and 10^6 yr (late accretion). The full list of parameters are given in Table 1.

Note that we have chosen an abrupt accretion model rather than a gradual accretion which is in order to model the Class 0 protostar (Smith 2000a).

Can protostars form via disk accretion? Turbulent viscosity in a disk is only efficient in the inner regions (e.g. Pringle 1987). This is shown in Figure 1 by the change in the profiles for the disk mass, viscosity and column which occurs at ~ 2 , 20 and 200 AU for the three ages. As shown in the Figure, a massive disk forms during the peak accretion phase. Turbulent viscosity is capable of processing this material onto the hydrostatic core only in the inner few AU. Viscosity through tidal forces, however, can negotiate the infall through the outer disk.

A nastier problem arises from the accretion time scale. The change in the imposed accretion rate is so rapid that the

outer disk cannot reach a steady state. The inner disk then lags behind, producing an extended gradual phase of energy release as the material falls on to the protostar. The constraint to model the Class 0 phase with a viscous disk is that the time scale for viscous accretion should be less than the imposed accretion time scale

$$t_{vis} = R^2/(\nu_t + \nu_g) < t_{in} = \dot{M}_a/\dot{M}_a. \quad (29)$$

This quantity is also displayed in Figure 1. However, as defined, t_{vis} is mathematically inappropriate exactly at the peak where we have instead taken the time scale $t_{in} = t_o/\alpha$ ($= 10^4$ yr in the example).

The result is that only the inner disk (< 10 AU) can keep up with the accretion rate at all stages. This implies that, if we wish to impose a supply rate on the central jet engine through a disk, then the centrifugal barrier (marking where radial infall is held up by angular momentum) cannot be larger than about 10 AU. *Larger circumstellar disks may be present but they are not accretion disks* in the sense of being able to supply the protostar with most of its fuel during the peak phase. At later phases, the drop in mass and fuel supply is delayed by the outer disk if the centrifugal barrier is larger than 20 AU. Hence the abrupt accretion from the envelope becomes a gradual supply on to the star.

We can thus take the inner radius of the envelope to be approximately fixed. We take here an inner radius of 100 AU for the envelope evolutions shown in Figures 2, 3 and 4 but note that for the envelope model the inner density and the optical depth scale as given by Equations 8 and 9. This implies, for example, that the optical depth of the envelope far exceeds unity to $\sim 10^6$ yr for a low mass protostar.

Note also that the turbulent ‘ α ’ takes, typically, 7000 years before it is extended to 1 AU, and that ‘Q-disks’, in which the tidal forces provide an effective viscosity, is crucial in transferring envelope mass to the α -disk during the peak accretion and transition phases (lower-left boxes in Figures 2, 3 and 4).

The disk temperature here follows the standard $T \propto R^{-3/4}$ law (Figure 1). Many T Tauri stars, however, possess disks which follow a flatter law (Adama, Lada & Shu 1987, 1988) thought to be caused by irradiation from light originating from the central star. The disk becomes cooler, less massive and thinner with time, but remains optically thick.

6. RESULTS: THE OUTFLOW EVOLUTION

Jets can be mainly molecular for an initial phase up to the peak accretion timescale of 10,000 years (lower-right boxes in the evolution figures). This is due to reformation at the jet base where high densities are encountered. After the peak, however, the jet density and the molecular content both fall rapidly. Hence, molecular jets may be associated with only the youngest Class 0 outflows. Later jets, however, could possess some molecular knots if the material is injected impulsively rather than smoothly, as assumed here.

A strong magnetic field is necessary if it is to drive the jets (see lower-central panels to the evolution figures). The derived magnetic field strengths are of order of a kilogauss during the peak accretion phase. The magnetic field may influence the properties of masers at radio wavelengths where we may best hope to observe through the envelope. The magnetic field drops very rapidly with time: the light jets being produced after 100,000 years are easily generated.

disk radial profile evolution

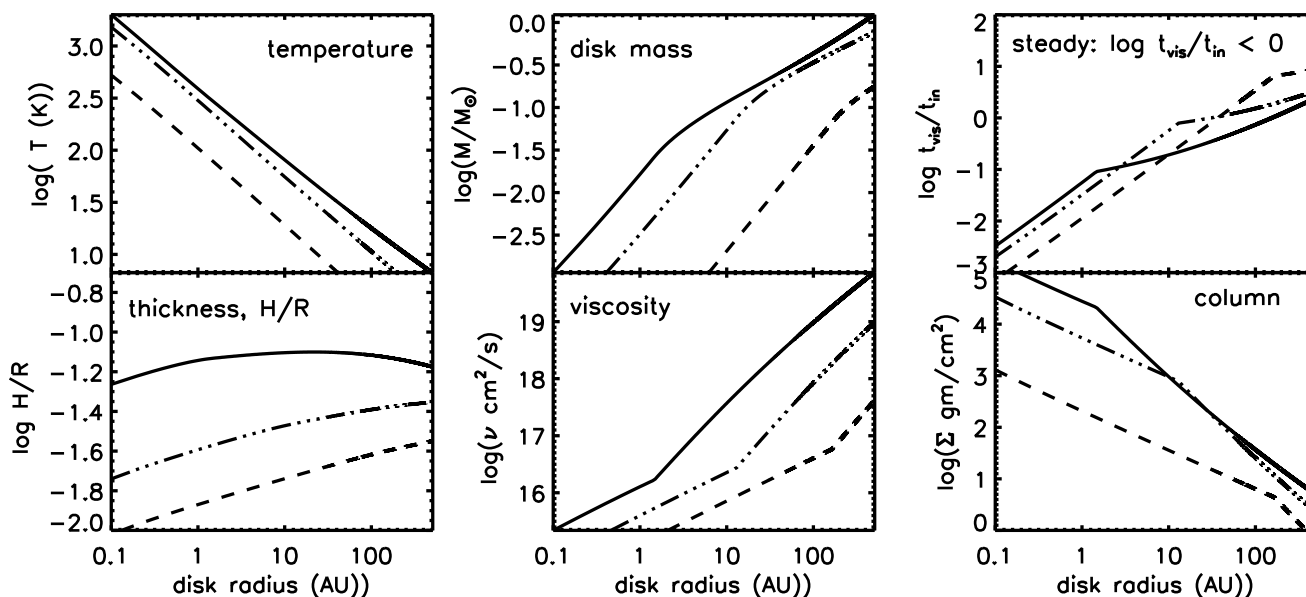


Fig. 1. Disk properties at 10^4 years (solid), 10^5 years (dot-dash) and 10^6 years (dash). Note that viscosity through gravitational forces takes over from turbulent viscosity in the outer disk, providing the kink.

The emission from shocks decreases extremely rapidly with time (see right-hand panels of the evolution figures). Shocked emission is produced instantaneously; the light jets cannot produce much shocked gas. Hence the infrared emission from molecules falls rapidly. Note that the shocks are mainly generated in the ambient cloud and so do not rely on the jets to be molecular. In contrast, the mechanical luminosity falls off slowly since the outflow lobes are gradually accumulated. The result is that the ratio of mechanical to shock luminosities is a sensitive measure of the protostellar age. Old protostars possess strong CO submillimetre lobes but very weak H_2 infrared luminosities.

Two peaks appear in the bolometric luminosity. The first, weaker peak is associated with the molecular jet phase. Then there is a phase in which the outflow momentum flow rate or ‘thrust’ is extremely high (centre-right panels). This is the peak mass accretion phase, and as shown by the thrust, can generate the prodigious Class 0 outflows. The second peak in the bolometric luminosity is caused by the return to a phase in which the jets are less efficient at expelling the energy. Hence the relative thrust reaches a minimum. The observational implications are best seen by studying the evolutionary tracks in the next section.

The outflow size is found to be 2-5 parsecs after 300,000 years (central panels). The ambient density was, of course, adjusted until reasonable source sizes were predicted. This ‘fixing’, however, does reduce the free predictions of the model. Given that the ambient medium on the large scale could have a wide range of densities, from 0.1 to 10^5 cm^{-3} , it becomes difficult to relate the size to the age. Furthermore, once an outflow has entered a low-density medium it may disappear from view as it expands. It is clear that a general evolutionary pattern for the large and old outflows may not be forthcoming.

7. EVOLUTIONARY TRACKS

Evolutionary tracking has aided many major advances in our knowledge of stellar evolution. On the Hertzsprung-Russell diagram, we plot temperature-luminosity paths. For protostars, where the star-to-be is hidden, only the envelope and outflow are directly observable. There are four parameters in use: mass M_{env} , bolometric temperature T_{bol} and total luminosity L_{bol} of the envelope, and the mechanical thrust F_{mech} of the outflow.

The tracks derived from the power-law mass accretion rate perform loops on the $F_{\text{CO}}-L_{\text{bol}}$ diagram (Figure 5). This contrasts with previous model predictions for the exponential model in which the tracks are horizontal, from left to right, before turning down to low F_{CO} and L_{bol} values.

Figure 5 helps us understand the enigmatic locations of the Class 0 sources. Not only do they lie above and to the left of the Class 1 sources, but many are mixed in with the Class 1s. The tracks derived here explain this behaviour, predicting that a protostar evolves both up (Class -1M) and down (Class 1M) a ‘pre-stellar’ main sequence, forming a left-leaning loop at the intermediate stage we term ‘Class 0M’ (M for Model, to distinguish theory and observation). Physically, better terms are 1: Rise Phase, 2: Peak Phase, 3: Decline Phase.

Barsony *et al.* (1998) employ an ‘evolutionary status’ diagram to plot their data (Figure 6). The Class 0 and 1 objects are not intermingled on this plot. The envelope mass is, of course, closer related to the Class definition than the outflow properties. Figure 6 shows that model protostar tracks also evolve unambiguously in this picture, in remarkable agreement. At the Peak Phase the tracks are notched here. These notches are indeed lined up with the Class 0 protostars. The potential proto brown dwarfs, however, would not be classified as Class 0 since they possess less massive (possibly optically thin) envelopes (as displayed in Figure 4).

early evolution of a solar mass star

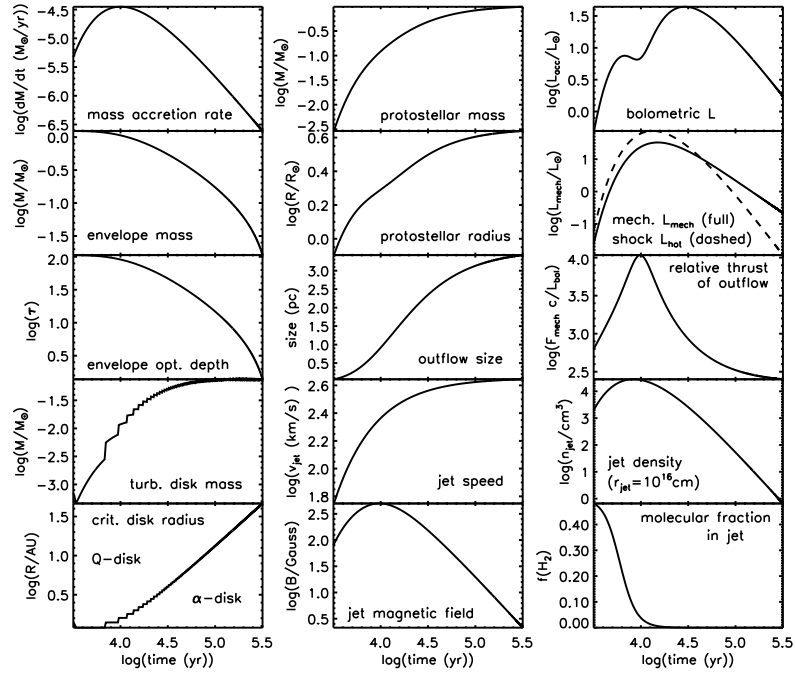


Fig. 2. From 3,000 to 300,000 years, a protostar which matures to a one solar mass star evolves as displayed. Logarithmic displays are required in most cases due to the wide ranges in variables and parameters. The set of constants are given in Table 1. An error in the jet density from Smith (2000b) has been corrected.

evolution of a low mass protostar

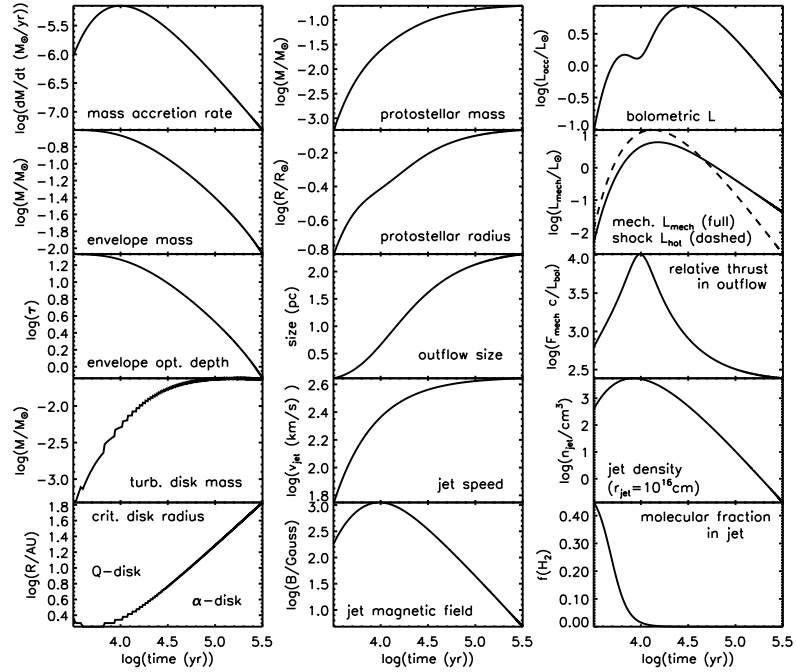


Fig. 3. From 3,000 to 300,000 years, a protostar which matures to a low mass star of $0.2 M_{\odot}$ evolves as displayed. The set of constants are given in Table 1.

evolution of a proto-brown dwarf

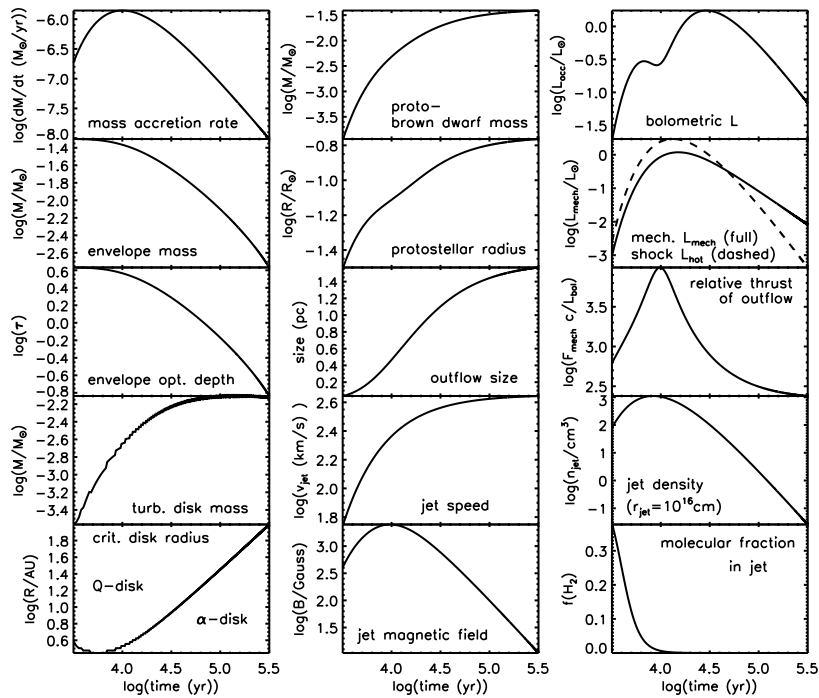


Fig. 4. From 3,000 to 300,000 years, a core which matures into a brown dwarf of $0.04 M_{\odot}$ evolves as displayed. The set of constants are given in Table 1.

The outflow momentum flux follows a closer correlation with the envelope mass than with the bolometric luminosity, according to a few studies (Saraceno *et al.* 1994, Hogerheijde *et al.* 1998). We display the correlation and the model tracks in Figure 7. The tracks we derive appear to provide an upper envelope as found in the observations. Furthermore, this diagram resolves part of the ambiguity of Figure 5 since the rising phase does not overlap with the declining phase.

For comparison, we have computed the thrust-luminosity diagram for the exponentially-decreasing accretion rate (Figure 8). Here, no sources are found in the early rise phase, and the highly-obscured Class 0 outflows coincident with the Class 1 protostars on this diagram appear out of place. In contrast, these Class 0 outflows could be associated with the early rise phase in the power-law model.

The displacement of the Class 1 sources below the tracks is not a critical problem: a factor of 2 overestimate of the thrust is easily possible, given that we have assumed that all the momentum is in the detected cool CO gas. A displacement is present for both exponential and power-law models.

8. CONCLUSIONS

A synchronised abrupt evolution with a power-law decrease in accretion rate has proved successful. Our results can be summarised as follows.

1. Evolutionary tracks relating the outflow thrust, envelope mass and bolometric luminosity characterise the model. The evolution begins with the outflow thrust increasing faster than the luminosity. Then, the luminosity rapidly increases while

the outflow thrust is constant. Finally, the envelope begins to be shed, as the outflow and luminosity then also decrease.

2. The power-law decreasing accretion rate generates looped tracks on the outflow thrust-bolometric luminosity diagram. A model with an exponentially-falling rate generates different routes which do not explain the present set of data.

3. Jets evolve from being heavy and molecular to light and atomic, assuming that the molecules only form in the base of dense, dusty jets. This implies that the early jets are ballistic and structure will be generated by pulsations and precession in the jet direction. Later jets are subject to external influence and structure is produced by surface instabilities.

4. The sizes of outflows are consistent with a synchronised evolution provided the mean ambient density is $\sim 10^{-3}$.

5. The ratio of instantaneous shock power to accumulated momentum is related to the ratio of molecular low-J CO and vibrationally-excited H_2 emission. At the peak accretion phase, the infrared shock emission is relatively strong, while in old sources a giant reservoir of CO gas may still be detectable.

6. Steady accretion disks are quite small, of order 10-20 AU since the mass accretion rate varies rapidly. Hence, a rapid accretion phase from the envelope to the disk would not produce a short high-thrust outflow unless the envelope is also small. If such envelopes are not constructable, we will have to pursue other means of supplying the jet engine during the Class 0 phase.

7. Proto Brown Dwarfs may be detectable through their substantial outflows. Their lower density envelopes may allow us to look deeper into these systems at an early formation stage, where we predict high magnetic fields.

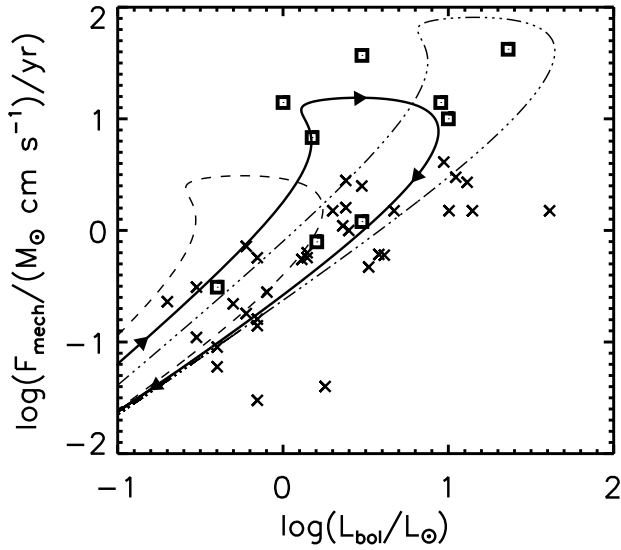


Fig. 5. The momentum flux - luminosity diagram for the 'power-law' accretion rate. The data is taken from Bontemps *et al.* (1996), Class 0 objects (squares) and Class 1 objects (crosses) are displayed. The evolutionary tracks lead to protostars of mass $1.0 M_{\odot}$ (dot-dash), $0.2 M_{\odot}$ (full) and $0.04 M_{\odot}$ (dash). For simplicity, error bars and a few upper limits have not been plotted. Chosen parameters are given in Table 1. An error in the jet density from Smith (2000b) has been corrected.

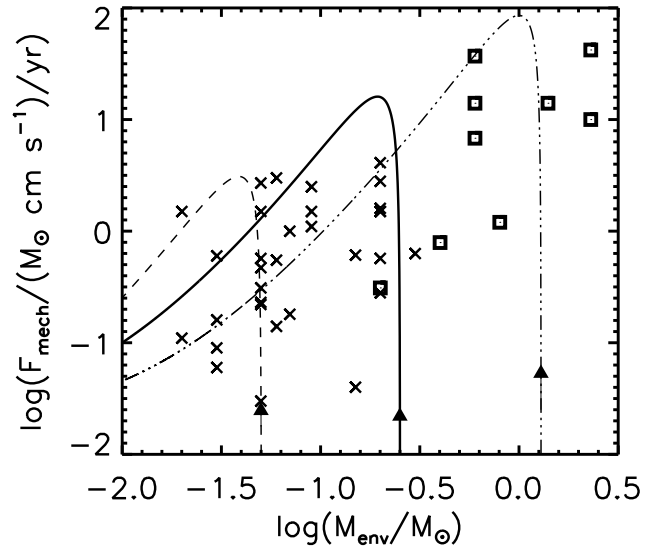


Fig. 7. The circumstellar or envelope mass - outflow diagram. The data is taken from Bontemps *et al.* (1996). Details are as in the caption for Figure 6.

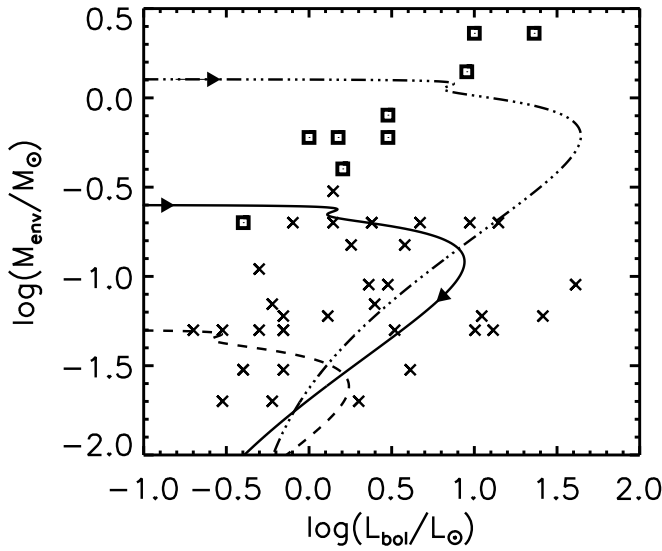


Fig. 6. The circumstellar or envelope mass - luminosity diagram. The data is taken from Bontemps *et al.* (1996), Class 0 objects (squares) and Class 1 objects (crosses) are displayed. The evolutionary tracks lead to protostars of mass $1.0 M_{\odot}$ (dot-dash), $0.2 M_{\odot}$ (full) and $0.04 M_{\odot}$ (dash). For simplicity, error bars and a few upper limits have not been plotted. Chosen parameters are given in Table 1.

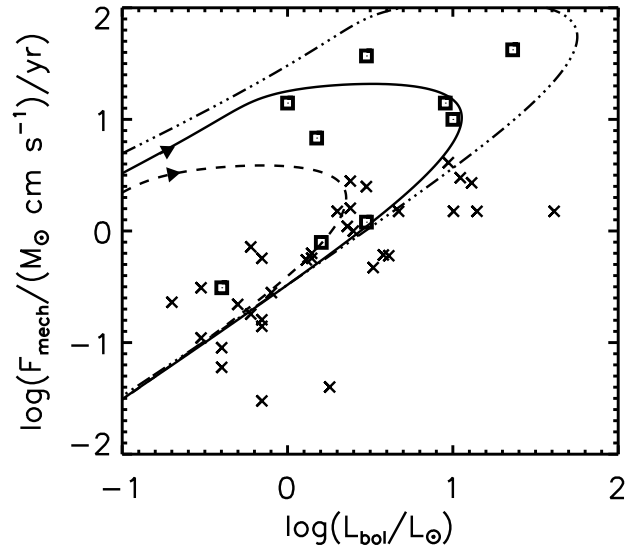


Fig. 8. The exponential law: momentum flux - luminosity diagram. The evolutionary tracks lead to protostars of mass $1.0 M_{\odot}$ (dot-dash), $0.2 M_{\odot}$ (full) and $0.04 M_{\odot}$ (dash). We chose $\tau_{ur} = 0.1$ and $\tau_f = 1.0$ in Equation 5.

References

- Adams F. C., Lada C. J., Shu F. H., 1987, *ApJ*, 321, 788.
 Adams F. C., Lada C. J., Shu F. H., 1988, *ApJ*, 326, 985.
 André P., Ward-Thompson D., Barsony M., 2000, in *Protostars & Planets IV*, V. Mannings, A. P. Boss & S. S. Russell (eds), University of Arizona Press, Tuscon, (in press).
 Bally J., Devine D., 1994, *ApJ*, 428, L65.
 Barsony M., Ward-Thompson D., André P., O'Linger J., 1998, *ApJ*, 509, 733.
 Bodenheimer P., 1992, in *Star Formation in Stellar Systems*, G. Tenorio-Tagle, M. Prieto & F. Sanchez (eds), Cambridge University Press.
 Bontemps S., André P., Terebey S., Cabrit S., 1996, *A&A*, 311, 858.
 Calvet N., Hartmann L. W., Strom S. E., 2000, in *Protostars & Planets IV*, V. Mannings, A. P. Boss & S. S. Russell (eds), University of Arizona Press, Tuscon, (in press).
 Davis C. J. *et al.*, 2000, *MNRAS*, (in press).
 Davis C. J., Smith M. D., Moriarty-Schieven G. H., 1998, *MNRAS*, 299, 825.
 Eislöffel J., Mundt R., 1997, *AJ*, 114, 280.
 Eislöffel J., Mundt R., Ray T. P., Rodriguez L. F., 2000, in *Protostars & Planets IV*, V. Mannings, A. P. Boss & S. S. Russell (eds), University of Arizona Press, Tuscon, (in press).
 Fendt C., Camenzind M., 1996, *A&A*, 313, 591.
 Foster P. N., Chevalier R. A., 1993, *ApJ*, 416, 303.
 Guenther E. W., Lehmann H., Emerson J. P., Staude J., 1999, *A&A*, 341, 768.
 Hartmann L. W., 1998, *Accretion Processes in Star Formation*, Cambridge University Press
 Henriksen R., André P., Bontemps, S., 1997, *A&A*, 323, 549.
 Hogerheijde M. R., van Dishoeck E. F., Blake G. A., van Langevelde H. J., 1998, *ApJ*, 502, 315.
 Königl A., Pudritz R. E., 2000, in *Protostars & Planets IV*, V. Mannings, A. P. Boss & S. S. Russell (eds), University of Arizona Press, Tuscon, (in press).
 Lada C. J., 1987, in *Star Forming Regions*, IAU Symp 115, M. Peimbert & J. Jugaku (eds), Dordrecht, Reidel, p1.
 Lin D. N. C., Pringle J. E., 1987, *MNRAS*, 225, 607.
 Lin D. N. C., Pringle J. E., 1990, *ApJ*, 358, 515.
 Myers P. C., Adams F. C., Chen H., Schaff E., 1998, *ApJ*, 492, 703.
 Pringle J. E., 1988, in *Formation & Evolution of Low Mass Stars*, A. Dupree & M. T. Lago (eds), p153.
 Reipurth B., Bally J., Devine D., 1997, *AJ*, 114, 2708.
 Richer J. S. *et al.*, 2000, in *Protostars & Planets IV*, V. Mannings, A. P. Boss & S. S. Russell (eds), University of Arizona Press, Tuscon, (in press).
 Saraceno P., André P., Ceccarelli C., Griffin M., Molinari S., 1996, *A&A*, 309, 827.
 Shakura N. J., Sunyaev R. A., 1973, *A&A*, 24, 337.
 Shu, F. H., 1977, *ApJ*, 214, 488.
 Shu F. H., Najita J., Ostriker E., Wilkin F., Ruden S., Lizano S., 1994, *ApJ*, 429, 781.
 Smith M. D., Suttner G., Yorke H. W., 1997, *A&A*, 323, 223.
 Smith M. D., 1999, *ApSS*, 261, 169, (Unification 1).
 Smith M. D., 2000a, in *Astrophysics and Cosmology: a collection of critical thoughts*, W. Kundt & C. van der Bruck (eds), Springer, Heidelberg (Unification 2).
 Smith M. D., 2000b, in *Optical and Infrared Spectroscopy of Circumstellar Matter*, S. Klose *et al.* (eds), ASP Conference Series, (in press).
 Völker R., Smith M. D., Suttner G., Yorke H. W., 1999, *A&A*, 343, 953.